Radar-observed Precipitation During NAME 2004

David A. Ahijevych
National Center for Atmospheric Research (NCAR)
ahijevyc@ucar.edu

Co-Authors:
Richard E. Carbone, NCAR
Timothy J. Lang, Stephen W. Nesbitt, Steven A. Rutledge, Colorado State University

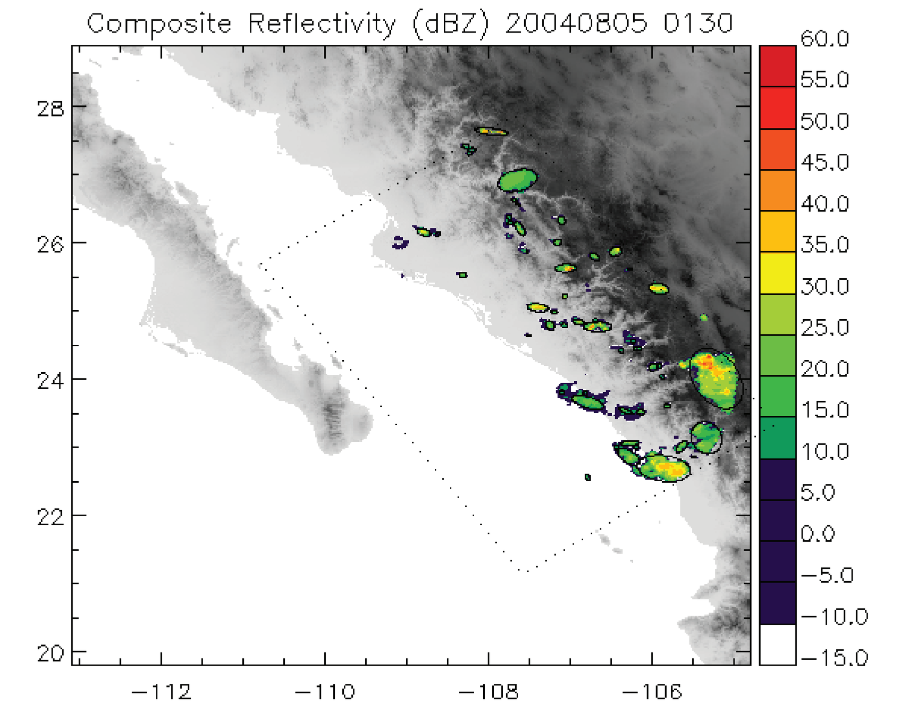

The Dataset

During July and August 2004, three Doppler radars (including the dual-polarized S-Pol radar) monitored the Tier 1 region of the North American Monsoon Experiment (NAME) near the mouth of the Gulf of California. This period just captured the initial onset of the monsoon along with intraseasonal variability due to Gulf Surges, easterly waves, break periods, and transients in the westerlies. A nearly continuous record of precipitation is now available from 0000 UTC, 8 July 2004, to 2345 UTC 21 August 2004.

Throughout the enhanced observing period, and among other types of scans, S-Pol provided one set of low-angle 360° surveillance scans (0.8°, 1.3°, and 1.8° elevation angles) for rain mapping, usually out to ~210 km range. Another set of scans extending to higher elevation angles was used for the analysis of precipitation vertical structure, but these data are not used in this study. Both scan sets were routinely updated every 15 minutes.

Reflectivity data from up to three different radars were merged into a network composite using the closest sweep in time to 00, 15, 30, and 45 minutes past the hour. Where sweeps overlapped, the lowest unblocked radar gate took precedence. Both 0.02 and 0.05 deg (~2 and ~5 km) grids were produced on a cylindrical projection. To reduce computing tme, the original spherical coordinate radar rays were interpolated to every 1 km in the radial. The resampled gates were then interpolated to lat-lon grids using an inverse-distance weighting method. Gates more than 0.04 deg (~4 km) from each grid point were assigned zero weight.

The latest composite products (version 2) are currently at http://data.eol.ucar.edu/master_list/?project=NAME. They supersede version 1, which was released to the community in 2005.

A new addition to the version 2 radar composite dataset is the corresponding satellite infrared brightness temperature. This field is adequate to discriminate between actual precipitation echo and sea clutter west of Cabos San Lucas.

Calibration

S-Pol:

Removed most AP, ground clutter, second-trip echo, and insect echoes with automated polarimetric thresholds.

Horizontal reflectivity (Z_h) and differential reflectivity (Z_{dr}) corrected for precipitation attenuation with differential phase shift.

Z_h corrected for gaseous attenuation.

Partial blockage quantified by comparing Zh to specific differential phase shift (K_{dp}) over a narrow range of (K_{dp}) for the entire experiment. K_{dp} is quite resistent to blockage effects, so a negative deviation of Zh from the empirical Zh-Kdp relationship can be ascribed to beam blockage. Corrections were applied as a function of azimuth and range.

Blockage-induced bias in Z_{dr} characterized by long-term non-zero mean in drizzle as a function of azimuth and range.

TRMM Precipitation Radar overpasses indicate mean Zh difference of only 0.06 dBZ from S-Pol corrected reflectivity.

Rainfall estimated with CSU blended algorithm based on Kdp, Zh, Zdr. and various combinations thereof.

Cabo and Guasave:

Removal of radar artifacts based on normalized coherent power, Zh, and total power thresholds. Required substantial manual intervention based on hand-editing.

Iterative correction technique applied to C-band Zh due to attenuation in precipitation.

Zh bias removed based on inter-comparison with S-Pol. This changed several times throughout the experiment.

Additional details in dataset README file.

Examples

these plots taken from 0.02 degree grid

Rainfall rate 6 Aug 2004 12:15 UTC
values here range from 0-80 mm/h

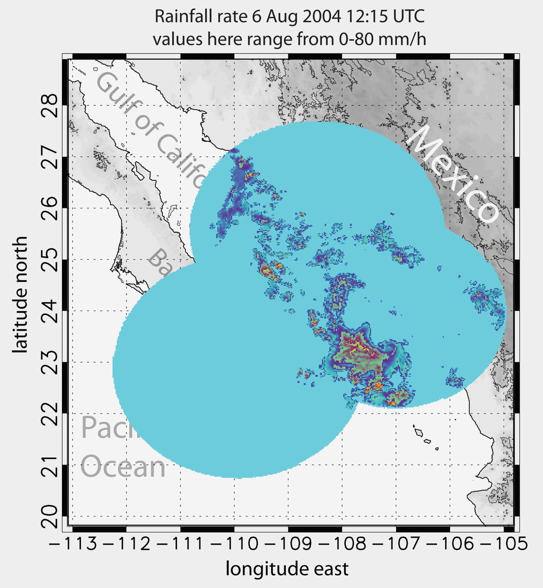

RR

Radar beam height 6 Aug 2004 12:15 UTC
values shown from 42-9500 m MSL (blue-dark red)

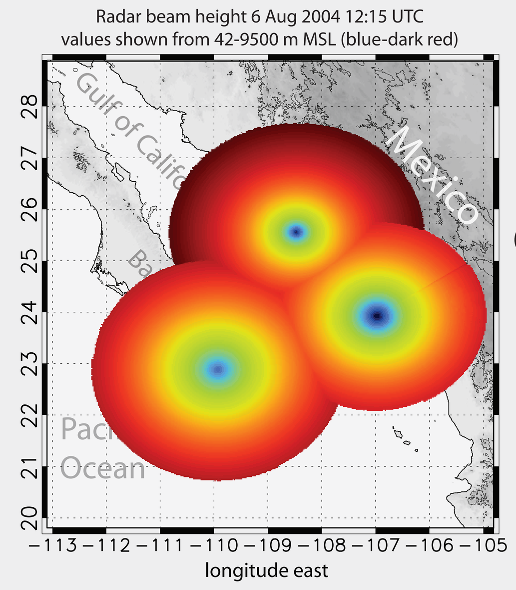

height_MSL

Satellite Infrared Brightness Temperature
26 Jul 2004 20:00 UTC 201-317 K (blue-red)

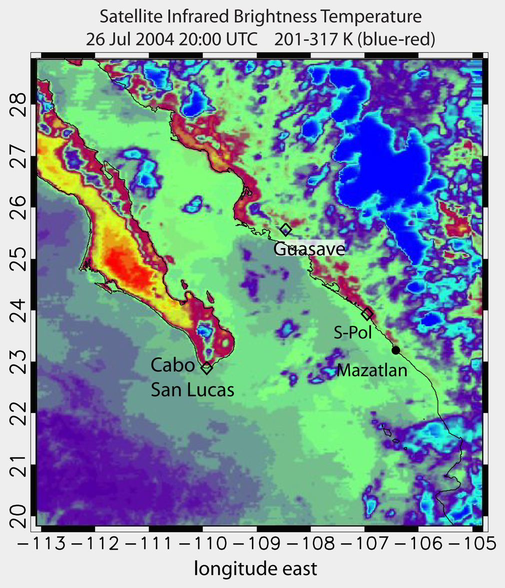

T_{BR}

Rainfall rate 6 Aug 2004 12:15 UTC
same as above except on 0.05 degree greid (~5km)

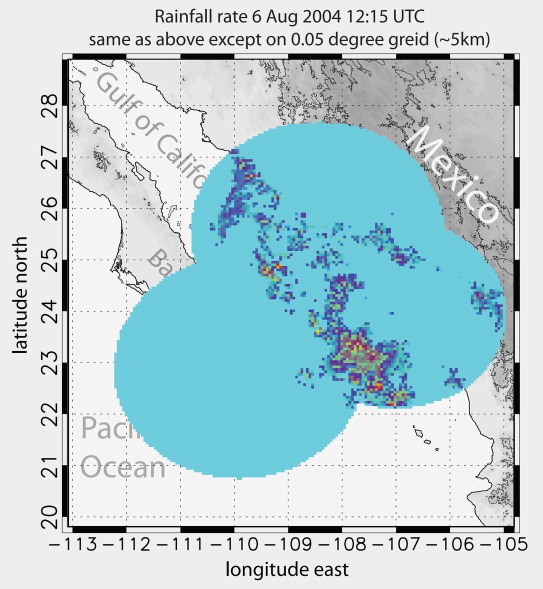

RR

Dates: July 8, 2004 - August 21, 2004
Navigation: latitude-longitude grid (0.02 and 0.05 degree spacing)
Format: netCDF

Constituent radars:

Los Cabos (Cabos San Lucas): C-band, Doppler, SMN (Sevicio Meteorological Nacional)

Guasave: C-band, Doppler, SMN

S-pol: S-band, Doppler, polarimetric (linear horizontal and vertical), NCAR

Fields available:

DZ: radar reflectivity factor (dBZ)

RR: rainfall rate (mm/h)

height_MSL: height of beam above mean sea level (m MSL)

TBR: satellite IR brightness temperature (K)

Reduced Dimension Analysis

In order to examine characteristics of the rainfall climatology, a reduced dimension analysis subdomain was created. The subdomain is aligned with the mean orientation of the SMO and the GoC, as illustrated below. The grid is rotated 35° counterclockwise from true north. Its orientation largely relegates the topographical and related surface variations to the x-dimension.

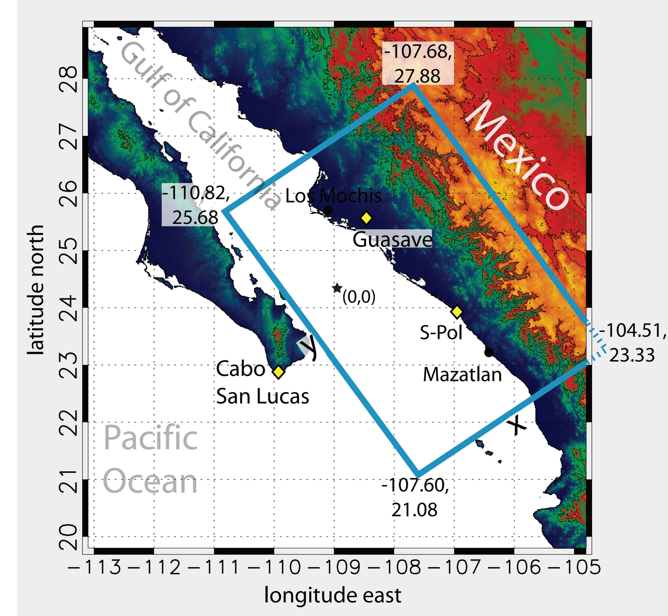

above: NAME radar composite domain with an inscribed sub-domain used for the reduced dimension analyses (blue rectangle). The origin (0,0) corresponds to the center of the radar composite.

below: The sub-domain and related terrain variations. Surface elevation is shaded and mean elevation profiles are shown along the sides. X-axis segments corresponding to the GoC, Coastal Plain, SMO Foothills, and SMO Peaks are labeled.

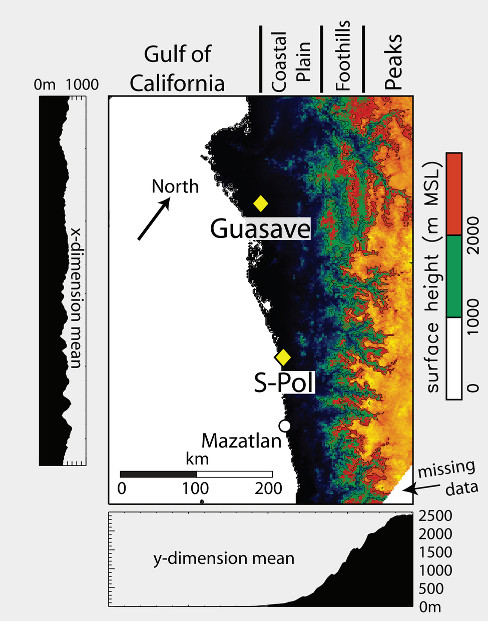

The analyses from this domain (right) are based on arithmetic averages of the radar-estimated rainfall rate along either the x- or y-dimension and subsequently plotted as a function of time (Hovmöller diagrams) at 15-min intervals. Where data are incomplete (meaning no radar was scanning at a particular grid point at a given time), at least 60 km of valid data (contiguous or not) must be present to calculate an average along any given gridline at any given time.

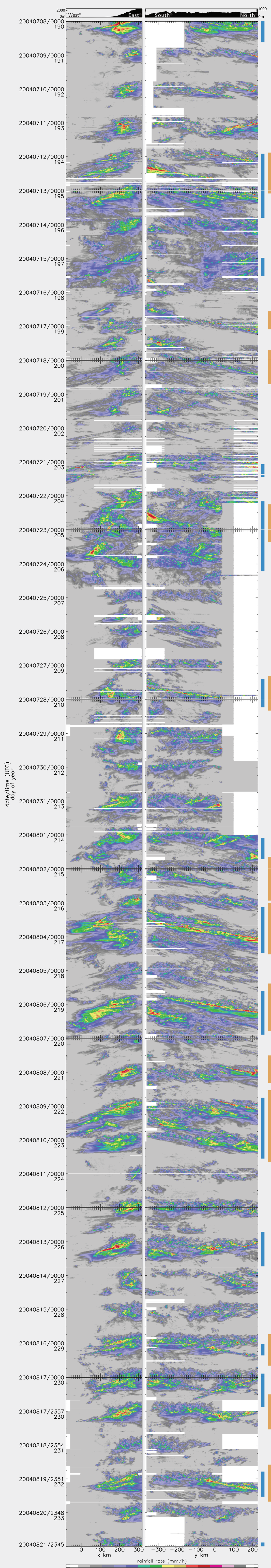

The Hovmoller diagram on the left shows the 45-day time series of average rainfall rate in reduced dimension, both transverse (l.h.s.) and parallel (r.h.s.) to the GoC/SMO major axis. Several characteristics are evident including:

- A pronounced diurnal cycle of rainfall over the period of record
- Horizontal patterns, indicating little movement of precipitation regions
- Smoothly sloping patterns, indicative of a systematic phase speed
- Tendency for major events to originate over SMO peaks and Foothills (l.h.s.)
- Phase speeds suggestive of slow movement from the SMO to the GoC (l.h.s.)
- Periods when precipitation progresses well into or across the GoC (l.h.s.)
- Periods when phase speeds exhibit consistent along-coast movement (r.h.s.)

The variability in precipitation patterns appears largely systematic. For pragmatic reasons, we identify two regimes to help characterize this variability. We have set an arbitrary threshold of 0.17 mm h-1 for the 24-h average rainfall over the GoC and coastal plain, above which Regime A is designated. As a consequence of this threshold, Regime A occurs one-third of the time. Regime A is characterized by a coherent progression of enhanced rainfall from the SMO to the GoC. Precipitation over the GoC is mainly nocturnal. A blue stripe along the right side marks the periods designated as Regime A. It is evident that other days exhibit a similar tendency for coherent progression of precipitation into the GoC under more suppressed conditions.

GoC regime (A) Along-coast propagation (B)

Regime B is defined when along-coast progression of precipitation is prominent. Along-coast progression of precipitation manifests itself as sloping rainfall streaks on the r.h.s. From previous studies (Carbone et al. 2002) in other regions it has been determined that the sloping rainfall streaks are often associated with organized mesoscale convection while the horizontal structures are characterized as unorganized convection. The orange stripe along the right side of Fig. 3 designates Regime B and indicates along-coast motion of ~10 m s-1.

Our identification of regimes is phenomenologically based. Further research is required to ascertain whether there is any physical or dynamical basis to the observed precipitation patterns. However, our initial results suggest that Regimes A and B are correlated with different wind shear environments, and not necessarily proximity to tropical easterly waves.

Diurnal Cycle

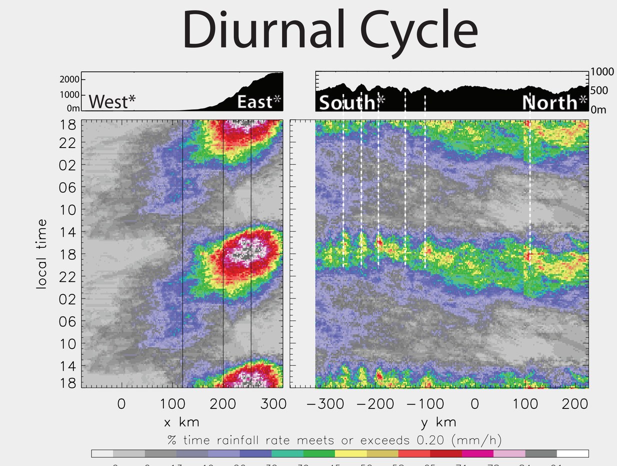

The percentage of time that rainfall meets or exceeds 0.2 mm h-1 is shown above as a function of x- or y-distance and time of day (LT) for the entire period of record. Note the maximum frequency of occurrence near 1800 LT over the SMO Peaks and Foothills (l.h.s.). The persistent triggering of afternoon convection in this region is indicated by the rapid onset of high precipitation frequencies around 1400. While the diurnal maximum is broad, a progression toward the GoC is evident: precipitation moves off the SMO, arrives on the coastal plain (x = ~100 km) around local midnight, and often persists until sunrise. After 0300, motion away from the SMO and into the GoC decreases significantly as evidenced by the frequency peak becoming diffuse with little appreciable change in the position of the centroid.

The along-coast diurnal cycle is shown on the right side of the above figure. Isolated maxima in precipitation frequency align with local peaks in the mean elevation profile. As in mid-latitude North America, elevated heat sources in the SMO play a dominant role in the excitation of deep moist convection (Carbone et al. 2002; Ahijevych et al. 2004). Another feature of significance is the along-coast trend of increasing nocturnal precipitation in the southern portion of the domain, where the coastal plain is narrow and a larger fraction of the x-dimension resides over the GoC.

References

Ahijevych, D. A., C. A. Davis, R. E. Carbone, and J. D. Tuttle, 2004: Initiation of precipitation episodes relative to elevated terrain. J. Atmos. Sci., 61, 2763-2769.

Carbone, R. E., J. D. Tuttle, D. A. Ahijevych, and S. B. Trier, 2002: Inferences of predictability associated with warm season precipitation episodes. J. Atmos. Sci., 59 (13), 2033-2056.

Lang, T. J., D. A. Ahijevych, S. W. Nesbitt, R. E. Carbone, S. A. Rutledge, and R. Cifelli, 2006: Radar-observed characteristics of precipitating systems during NAME 2004. J. Climate. Special Issue on the North American Monsoon Experiment. In press.